Characterization of a Condenser for a High Performance Multi-Condenser Loop Heat Pipe

Citation: Hanks, Daniel F., Teresa B. Peters, John G. Brisson, and Evelyn N. Wang. "Characterization of a Condenser for a High Performance Multi-Condenser Loop Heat Pipe." Volume 10: Heat and Mass Transport Processes, Parts A and B (2011).

As Published: http://dx.doi.org/10.1115/IMECE2011-63250

Publisher: ASME International

Persistent URL: http://hdl.handle.net/1721.1/119174

Version: Final published version: final published article, as it appeared in a journal, conference proceedings, or other formally published context

Proceedings of the ASME 2011 International Mechanical Engineering Congress & Exposition
IMECE2011
November 11-17, 2011, Denver, Colorado, USA

IMECE2011-63250

CHARACTERIZATION OF A CONDENSER FOR A HIGH PERFORMANCE MULTI - CONDENSER LOOP HEAT PIPE

Daniel F. Hanks, Teresa B. Peters, John G. Brisson, and Evelyn N. Wang
Department of Mechanical Engineering
Massachusetts Institute of Technology
Cambridge, MA 02139
Email: dhanks@mit.edu

ABSTRACT

We experimentally characterized a condenser design for a multi-condenser loop heat pipe (LHP) capable of dissipating 1000 W. The LHP is designed for integration into a high performance air-cooled heat sink to address thermal management challenges in advanced electronic systems. The multi-layer stack of condensers utilizes a sintered wick design to stabilize the liquid-vapor interface and prevent liquid flooding of the lower condenser layers in the presence of a gravitational head. In addition a liquid subcooler is incorporated to suppress vapor flashing in the liquid return line. We fabricated the condensers using photochemically etched Monel frames with Monel sintered wicks with particle sizes up to 44 μm. We characterized the performance of the condensers in a custom experimental flow rig that monitors the pressure and temperatures of the vapor and liquid. The condenser dissipated the required heat load with a subcooling of up to 18 °C, while maintaining a stable liquid-vapor interface with a capillary pressure of 6.2 kPa. In the future, we will incorporate the condenser into a loop heat pipe for a high performance air-cooled heat sink.

INTRODUCTION

The performance and reliability of computing today is limited by the rate at which thermal energy can be rejected from a microprocessor. Additionally, the electricity demand of all data centers in the United States accounts for 5%-10% of our total electricity consumption and half of this power is consumed by the cooling systems [1]. Thermal management solutions are needed to efficiently and reliably dissipate high thermal loads from CPUs.

The proposed device in Fig. 1 incorporates a loop heat pipe (LHP) with a single evaporator and multiple flat-plate air-cooled

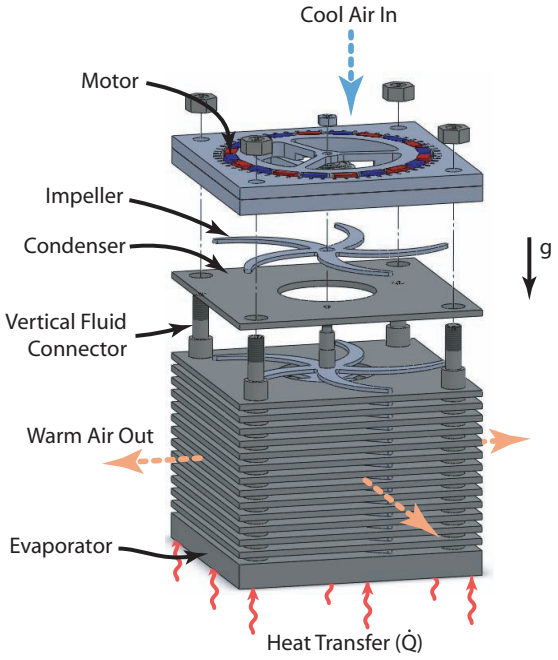

FIGURE 1. Schematic of integrated heat sink: impellers are interdigitated between condensers of the loop heat pipe.

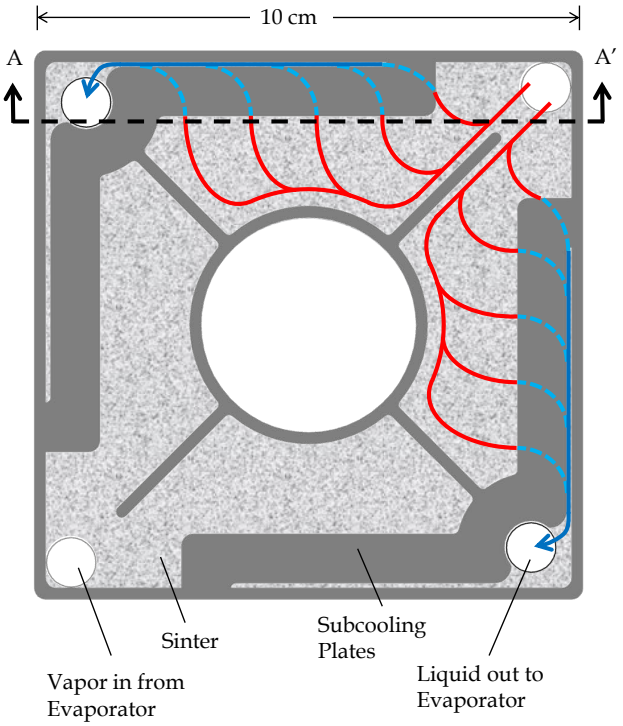

FIGURE 2. Schematic showing inside of condenser where vapor condenses on the sinter and the liquid flows under subcooling plates. Red and blue represent vapor and liquid flow, respectively.

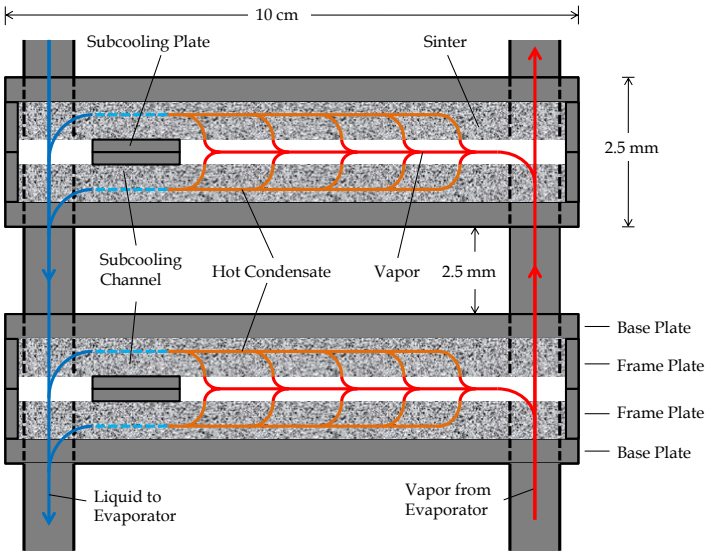

FIGURE 3. Schematic of cross-section AA' of two representative condensers. Vapor (red) condenses onto the sinter where saturated liquid (orange) flows through the sinter. The liquid is subcooled (dashed blue) and is then recirculated (dark blue) back to the evaporator. Note: schematic not to scale.

condensers. The integrated design aims to dissipate 1000 W from a heat source at 80 °C to ambient air at 30 °C using 33 W of input electrical power. These requirements correspond to an overall thermal resistance of 0.05 °C/W and a coefficient of performance (COP) of 30. Furthermore, to easily integrate such a cooling device in several applications, the heat sink needs to be contained in a compact space of 10x10x10 cm and be capable of operating in any orientation. Because the system's largest thermal resistance is associated with convection to ambient air, 1.5 mm thick impellers are interdigitated between the condensers which are spaced 2.5 mm apart, leaving 0.5 mm between the impeller and condenser surface. This arrangement leads to high convective heat transfer coefficients due to shearing of fluid boundary layers and developing flow in the gap between condensers [2]. This impeller design combined with a low temperature drop ($\sim 3°C$) between the evaporator and the condensers leads to a near isothermal condenser surface and maximal temperature drop to ambient air.

Water is chosen as the working fluid in the LHP due to its high latent heat of vaporization and surface tension. Because liquid flow passages in an LHP are smooth and contain no wick, condensate must be subcooled to prevent it from spontaneously vaporizing [3]. To prevent vaporization in the liquid return line, a liquid subcooler is incorporated into each condenser layer as depicted in Fig. 2. The red lines in Fig. 2 represent vapor, the dashed blue lines represent liquid being actively subcooled and the blue lines represent subcooled liquid. Figure 3 is a cross section of two condensers from the dashed line marked AA' in Fig. 2. Condensate is able to be subcooled because vapor is blocked from the subcooling channels by a solid Monel subcooling plate. The LHP utilizes two vapor transport lines and two liquid transport lines which also provide structure for the LHP assembly and top-mounted motor shown in Fig. 1. Cool air is drawn in from the top and blown radially outwards between each condenser.

The vertical stacking of multiple condensers introduces new challenges to the LHP design. The gravitational pressure head of a 10 cm column of liquid condensate returning to the evaporator is 1.0 kPa. This pressure is sufficient to cause lower condenser layers to flood thereby inhibiting their capacity to condense vapor. Likewise if the heat pipe were inverted, there would be flooding of upper layers. To prevent this instability, a sintered wick is incorporated into the condenser to stabilize the liquid-vapor interface using capillary forces. The stability of the vapor-liquid interface at a wick surface depends on the difference of pressures between the liquid and vapor. As long as the capillary forces of the interface can compensate for the pressure differences, the interface will be stable. If the pressure in the liquid is higher than in the vapor, then the fluid menisci between the sintered particles will bulge into the vapor space, referred to here as an advancing meniscus. Similarly, if the pressure in the liquid is lower than in the vapor, then the menisci will bulge into the sinter, referred to here as a receding meniscus. Measurements

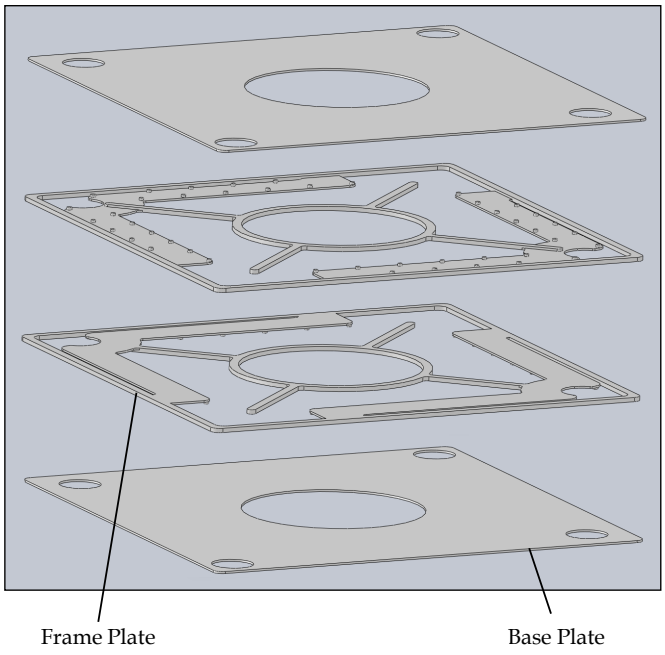

FIGURE 4. Exploded view of condenser consisting of four photo-chemically etched plates that are brazed together to from fluid channels.

performed on candidate sinters have shown that the maximum pressure sinters are able to sustain across the interface without flow (i.e., break-through pressure or ΔP_{max}) are larger in the receding direction than in the advancing direction [4]. To take advantage of this effect and improve on the safety margin of the design against condenser flooding, the liquid side of the condenser needs to operate at a pressure that is more than 1.0 kPa lower than the vapor side. Such a requirement will be achieved using a compensation chamber to set the liquid side pressure. The details of the compensation chamber are not discussed here.

Due to the decreased liquid side pressure, condensate must be subcooled relative to the reduced local saturation pressure on the liquid side. A large break-through pressure and a large amount of liquid subcooling are desired to provide a safety factor against liquid-vapor interface instability and against vapor appearing in the liquid return line.

This paper outlines the fabrication and characterization of a single condenser for use in a multi-condenser LHP. The condenser demonstrated stable operation with subcooling up to 18 °C and a maximum imposed pressure drop up to 14 kPa.

FABRICATION

The sinter and solid components of each condenser are fabricated from Monel 400 alloy which has high resistance to corrosion. To manufacture thin (0.5-0.75 mm) Monel parts with high precision, such as the part in Fig. 2, sheets of Monel are photo-chemically etched to varying depths. This design allows for a space under the subcooling length where condensate can flow. Each condenser is made from four photo-chemically etched plates of two types: a base plate (0.5 mm thick) and frame plate (0.75 mm thick) shown in Fig. 4. Note that the subcooling plate is a sub-component of the frame plate. The subcooling plate is elevated by 0.5 mm to create the subcooling channel as shown in Fig. 3.

The condenser is assembled by a series of furnace brazing and sintering steps at successively lower temperatures. First two half-condensers are assembled. The base plate is bonded to the frame plate with silver at 970 °C. The base plate and frame plate provide structure for the condenser and a cavity to contain the sintered wick. Next 44 μm Monel powder is poured into the frame and spread under the subcooling plate. To allow for a vapor space, 0.25 mm of powder is scraped off the surface. The powder is sintered at 820 °C for 12 minutes. The two halves are joined with a eutectic AgCu (72% Ag, 28% Cu) braze alloy at 810 °C. Multiple condensers are simultaneously brazed onto 9.5 mm (0.375") diameter Monel tubes for transporting liquid and vapor with 60% Ag, 30% Cu, 10% Sn braze alloy at 750 °C. To complete the heat pipe assembly, the tubes leading from the stack of condensers are attached to the evaporator with 80% Au, 20% Sn braze alloy at 330 °C.

The particle size, material and temperature for sintering Monel wick were chosen based on an experimental study of different types of sinter. The 44 μm non-spherical Monel powder yielded the most favorable properties including a bulk permeability of $\kappa = 1.5\pm0.2$ x10^{-12}m^2, a maximum break-through pressure of $\Delta P_{max} = 18.6\pm3.0$ kPa, and a bulk thermal conductivity of $k = 2.3\pm0.2$ W/m-K [5].

The most significant challenge in the fabrication was in achieving a reliable bond between the sintered wick and solid Monel. During the heating process, sintered wicks tend to shrink and even detach from adjacent walls. When the sintered wick detaches from the solid Monel around the subcooling channel, the resulting gaps can lead to a reduced break-through pressure.

A capillary pressure test was performed on an open-faced half-condenser by sealing it with a rubber gasket, flooding the condenser, and pressurizing air on one side of the subcooling channel until bubbles burst through the subcooling channel. The test demonstrated that such defects were indeed present and limited the break-through pressure to 6.2 ± 0.1 kPa. The presence of defects also led to a slight increase in permeability of the porous wick.

EXPERIMENTAL SETUP

A single condenser was experimentally characterized and evaluated for integration in a multi-condenser LHP. The primary objectives were to measure the condensation rate, the degree of liquid subcooling and ensure that the liquid-vapor interface re-

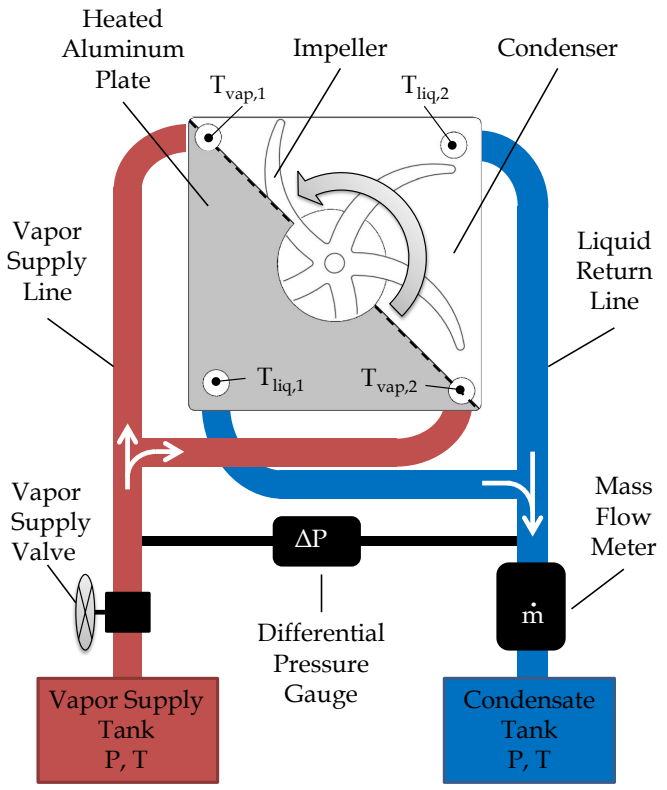

FIGURE 5. Experimental Setup. Vapor flows into the condenser which is cooled by an impeller-driven air flow. Liquid exits the condenser to a condensate tank which is fixed to a pressure lower than the pressure in the vapor supply.

mained stable during operation with a large imposed pressure drop between the vapor space and the liquid channel.

As shown in Fig. 5, a vapor supply tank with an attached band resistive heater (not shown) generates vapor at the desired temperature and pressure of 80 °C and 47 kPa. The vapor flows into the condenser via two vapor inlets on the bottom side. Condensate flows out of the condenser via two liquid outlets and subsequently through a calorimetric mass flow meter (TURCK FCI-TCD04A4P-LIX-H1141) before returning to a condensate tank which is immersed in a temperature control bath used to adjust the condenser outlet pressure. The difference in pressure between the vapor entering the condenser and the liquid flowing out of the condenser, ΔP, is measured using a differential pressure gauge (Honeywell FDW 060-M838-02) with an uncertainty of ± 0.1 kPa. The vapor and liquid temperatures at all four tube connections were measured by thermocouples (Omega TMQSS-062G-3) positioned in the fluid flow channel, each with an uncertainty of ± 0.5 °C and are indicated by T in Fig. 5. To simulate the cooling mechanism of the multi-layer device, an impeller rotates at 5000 rpm on each side of the condenser. Adjacent to each impeller is a heated aluminum square plate which is cut away in Fig. 5 to reveal the impeller underneath. The heated aluminum plate simulates the flow constriction and heat input of adjacent active condensers on each side of the experimental one. Each plate is heated with 50 W and insulated on the side opposite to that of the spinning impeller.

Non-condensable gases impede heat transfer in a condenser because the transport of vapor to the condensation surface is limited by diffusion [6]. Therefore, the use of de-gassed water as the working fluid and vacuum tight seals are essential. The most effective method for removal of non-condensable gases is the freeze-pump-thaw cycle [7]. Because gases have low solubility in ice, freezing the water causes the release of non-condensable gases. The vapor supply tank is filled with water, frozen, and the ice is then pumped to vacuum to evacuate released non-condensable gases. Since some non-condensibles can be trapped in the crystalline structure of ice (though not actually dissolved), the ice is thawed and the cycle is performed two more times or until the tank pressure and temperature match by saturation conditions.

After all freeze-pump-thaw cycles are complete, the condenser and all connected pipes are pumped down to vacuum. The de-gassed water in the vapor supply tank is heated to 80 °C and the empty condensate tank is also heated to 80 °C. The vapor supply valve is opened and steady state is reached after water fills the liquid pipes and enough water enters the evacuated condensate tank to satisfy saturation conditions. While the vapor supply is maintained at 80 °C, the temperature and thus the pressure in the condensate tank is gradually lowered to impose a pressure drop, ΔP, across the condenser. The pressure drop is increased until vapor penetrates through the sintered subcooling channel and into the liquid pipe, indicating a failure of the condenser.

RESULTS & DISCUSSION

Figure 6 shows characteristic experimental results of temperature and pressure data as a function of time. Figure 6 (a) shows the measured inlet vapor temperature (T_{vap}), each of the measured outlet temperatures (T_{liq}), and the calculated saturation temperature at the liquid outlet ($T_{sat,out}$) as functions of time. The liquid outlet saturation temperature was found by converting the saturated vapor inlet temperature to its corresponding saturated pressure, subtracting ΔP from this value, and calculating the saturation temperature corresponding to that pressure, or

$$T_{sat,out} = T_{sat}\left(P_{sat}(T_{vap}) - \Delta P\right) \tag{1}$$

Figure 6 shows that the temperature of vapor entering each inlet of the condenser has a constant value of $T_{vap} = T_{vap,1} = T_{vap,2} = 79.1 \pm 0.3$ °C. Figure 6 (b) shows the imposed pressure drop, ΔP, between the vapor inlet and liquid outlet as measured by the differential pressure gauge as a function of time. The periodic oscillations in T_{vap} and ΔP are due to the band heater on the vapor supply tank turning on and off. From Eq. 1, since

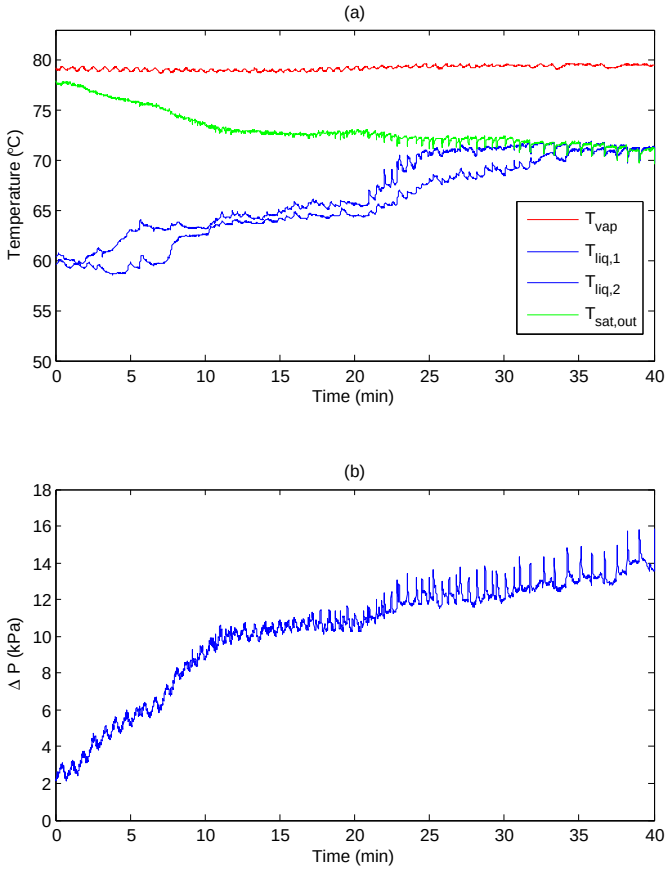

FIGURE 6. (a) The temperature of the liquid exiting the condenser (blue lines) rises to meet the saturation temperature(green line). The vapor temperature (red) is nearly constant. (b) The corresponding differential pressure also rises.

the vapor temperature and pressure remain constant, the change in ΔP varies inversely to the change in $T_{sat,out}$, the local liquid outlet saturation temperature. The differences in the two liquid outlet temperatures is likely due to variability in the two porous subcooling channels caused by defects in sinter bonding to solid Monel walls.

The trends in temperature and pressure over time clearly demonstrate the functionality of the condenser. Vapor is always entering the condenser in each vapor line while only liquid is exiting the liquid lines for the first 20 minutes of the experiment as the pressure drop ΔP increased.

An important factor for maintaining stable operation of the LHP is the liquid subcooling, ΔT_{sc}, which is the difference between the liquid outlet saturation temperature and actual liquid outlet temperature:

$$\Delta T_{sc} = T_{sat,out} - T_{liq} \tag{2}$$

The average of the two liquid outlet temperature was used for T_{liq} in calculating ΔT_{sc}.

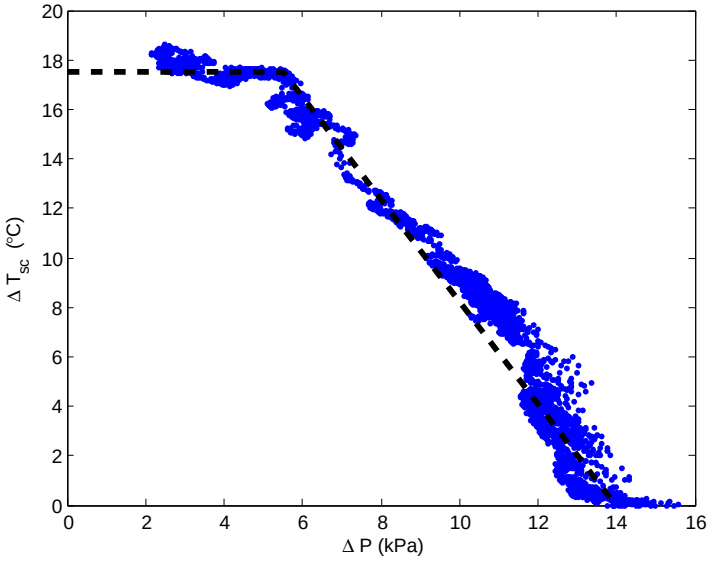

FIGURE 7. The change in liquid temperature (ΔT_{sc}) due to subcooling as a function of the differential pressure (ΔP).

Although vapor may be expected in the liquid line after the total pressure drop surpassed the break-through pressure of 6.2 kPa, the liquid remained subcooled. The level of subcooling in Fig. 7 was observed to gradually decrease with increasing pressure drop until ΔP = 14 kPa. This gradual failure can be explained by the two phase flow through the sintered wick as shown in Fig. 8. The change in temperature due to subcooling, ΔT_{sc}, should be an exponential function of the time that liquid spends flowing under the subcooling plate, though in this case it can be approximated as a linear function. At pressures below 6.2 kPa, the liquid-vapor interface is stable at the designed location, filling the entirety of the sintered subcooling channel with liquid. When the pressure drop rises above the break-through pressure of 6.2 kPa, the liquid-vapor interface recedes. As it recedes, low density vapor begins to flow through the low permeability sinter yielding a large viscous pressure drop as shown in Fig. 8. The vapor is prevented from reaching the liquid outlet as it is cooled by the sinter and mixes with subcooled liquid but the temperature of the exiting liquid increases, i.e. ΔT_{sc} decreases. As the pressure drop continues to increase, the liquid-vapor interface recedes even more and vapor penetrates further into the subcooling channel, causing a more significant decrease in subcooling. Eventually ΔT_{sc} is reduced to zero and vapor and liquid coexist in the liquid return line which would cause the LHP to fail.

By conservation of energy, the heat dissipated by the condenser can be calculated using the mass flow of condensate. Vapor entering the condenser at saturation transfers its latent heat of vaporization to the condenser as it changes to the liquid phase. The liquid transfers more heat to the condenser as it is subcooled. Equation 3 captures the transfer of heat from the working fluid

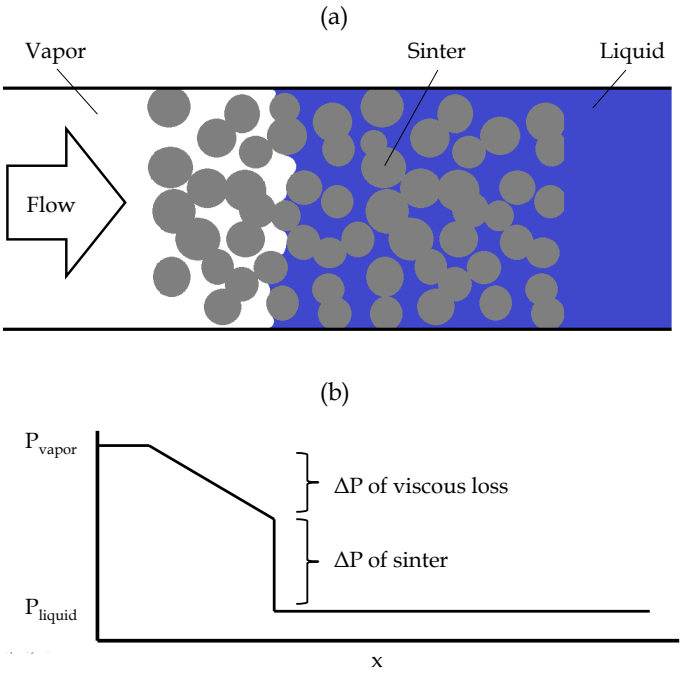

FIGURE 8. (a) Schematic showing liquid recession through sinter and (b) corresponding pressure drops. As the pressure drop increases, vapor penetrates into the sintered subcooling channels, while experiencing a viscous pressure drop. As a result, the amount of subcooling decreases.

to the condenser:

$$\dot{Q} = \dot{m}(h_{fg} + c_p(T_{vap} - T_{liq})) \tag{3}$$

where $\dot{Q}$ is the rate of heat transfer, $\dot{m}$ is the mass flow rate, h_{fg} is the latent heat of vaporization, and c_p is the specific heat of the liquid at constant pressure. The heat loss associated with subcooling is small compared to the latent heat loss. This method of measuring heat rejection also accounts for heat loss through all pipes where vapor is condensing, however all pipes were well insulated during the experiment. Because heat rejection for each condenser is governed by air convection factors such as geometry and impeller speed, the flow of condensate should be constant during the entire experiment. The data for condensate mass flow was consistent with this assumption during the experiment and averaged 0.043±0.015 g/s which corresponds to a heat loss of 101±36 W for the condenser. With sufficient airflow, an array of 14 condensers as shown in Fig. 1 can reach 1000 W total heat dissipation [8].

CONCLUSION

We successfully designed, fabricated, and tested single condensers for a multi-condenser heat pipe. The maximum pressure drop sustained by the condenser was greater than the break-through pressure because of an added viscous pressure drop as vapor flowed through the sinter. Condensate was subcooled by up to 18 °C and the liquid-vapor interface was stabilized for imposed pressure drops up to 14 kPa, allowing the heat pipe to operate under a gravitational pressure.

NOMENCLATURE

c_p specific heat of liquid at constant pressure, J/g-K
h_{fg} enthalpy of vaporization, J/g
κ permeability, m^2
k thermal conductivity, W/m-K
$\dot{m}$ mass flow rate, kg/s
P pressure, kPa
ΔP difference in pressure between liquid and vapor, kPa
ΔP_{max} maximum ΔP or break-through pressure, kPa
$\dot{Q}$ heat dissipation, W
T temperature, °C
T_{liq} temperature of liquid exiting the condenser, °C
$T_{sat,out}$ saturation temperature at condenser outlet, °C
T_{vap} temperature of vapor entering the condenser, °C
ΔT_{sc} subcooling temperature, °C

ACKNOWLEDGMENT

This work is supported by the Defense Advanced Research Projects Agency (DARPA) Microsystems Technology Office (MTO) Microtechnologies for Air-Cooled Exchangers (MACE) program, Grant Number W31P4Q-09-1-0007, with Dr. Tom Kenny and Dr. Avi Bar-Cohen as program managers.

REFERENCES

[1] Pop, E., 2010. "Energy dissipation and transport in nanoscale devices". *Nano Research,* ***3***(3), pp. 147–169.
[2] McCarthy, M., 2010. "Design and analysis of high-performance air-cooled heat exchanger with an integrated capillary-pumped loop heat pipe". In ITHERM.
[3] Faghri, A., 1995. *Heat Pipe Science And Technology*. Taylor & Francis Group.
[4] Kariya, H. A., 2010. Private Communication.
[5] Dominguez-Espinosa, F. A., To be published 2011. "Effect of fabrication parameters on thermophysical properties of sintered wicks". Master's thesis, Massachusetts Institute of Technology.
[6] Mills, A. F., 1999. *Basic Heat and Mass Transfer*, 2nd ed. Prentice Hall.
[7] Koveal, C. H., 2010. "Design of parallel plate condensers with sintered wicks for a loop heat pipe". Master's thesis, Massachusetts Institute of Technology.
[8] Staats, W. L., 2010. "Investigation of a multiple impeller design for a high performance air-cooled heat sink". In IMECE.